Uncovering the Enzymes that Catalyze the Final Steps in Oxytetracycline Biosynthesis

Peng Wang,[†] Ghader Bashiri,[‖] Xue Gao,[†] Michael R. Sawaya,[‡,§] and Yi Tang*[,†,‡]

[†]Department of Chemical and Biomolecular Engineering, [‡]Department of Chemistry and Biochemistry, and [§]UCLA-DOE Institute for Genomics and Proteomics, University of California Los Angeles, Los Angeles, California 90095, United States

[‖]Structural Biology Laboratory, Maurice Wilkins Centre for Molecular Biodiscovery and School of Biological Sciences, The University of Auckland, Auckland, New Zealand

S *Supporting Information*

ABSTRACT: Tetracyclines are a group of natural products sharing a linearly fused four-ring scaffold, which is essential for their broad-spectrum antibiotic activities. Formation of the key precursor anhydrotetracycline **3** during oxytetracycline **1** biosynthesis has been previously characterized. However, the enzymatic steps that transform **3** into **1**, including the additional hydroxylation at C5 and the final C5a−C11a reduction, have remained elusive. Here we report two redox enzymes, OxyS and OxyR, are sufficient to convert **3** to **1**. OxyS catalyzes two sequential hydroxylations at C6 and C5 positions of **3** with opposite stereochemistry, while OxyR catalyzes the C5a−C11a reduction using F_{420} as a cofactor to produce **1**. The crystal structure of OxyS was obtained to provide insights into the tandem C6- and C5-hydroxylation steps. The substrate specificities of OxyS and OxyR were shown to influence the relative ratio of **1** and tetracycline **2**.

T etracyclines are a group of aromatic polyketide natural products produced by soil-borne bacteria.[1] Their broad-spectrum antibiotic activities led to the widespread usage as front line antibiotics. The emergence of resistant mechanisms reduced the effectiveness of tetracyclines, leading to the continual demand for semisynthetic analogs that can overcome resistance mechanisms.[2] As biosynthetic targets, the oxytetracycline **1** (*oxy*) and tetracycline **2**/chlorotetracycline **4** (*ctc*) pathways have been investigated using genetic and biochemical approaches.[3] The biosynthesis of both **1** from *Streptomyces rimosus* and **2** from *Streptomyces aureofaciens* is known to go through the common, late intermediate anhydrotetracycline **3**. Although it is known that the anhydrotetracycline hydroxylase present in each pathway (OxyS and Cts8) is responsible for the (S)-hydroxylation of C6 in **3**,[4] the enzymatic basis of the remaining steps, including the additional hydroxylation of C5 in **1**, and the common C5a−C11a reduction that carves out the tetracycline structures are unclear (Figure 1). These steps are essential in sculpting the keto−enol containing lower periphery of tetracyclines, which is a critical feature in chelation of Mg^{2+} and binding to the 30S ribosomal subunit.[5] Understanding the enzymology behind these transformations is therefore needed to complete our knowledge of the tetracycline biosynthetic pathway as well as

toward the generation of new analogs based on this privileged scaffold using synthetic biology approaches.

The final C5a−C11a reduction step has been proposed to involve a F_{420}-dependent tetracycline dehydrogenase, in which intermediates **6** or **7** are reduced to **2** or **1**, respectively.[6] An earlier study proposed that the enzyme TchA encoded outside of the *ctc* gene cluster in *S. aureofaciens* is involved in this final reduction step of chlorotetracycline **4** (as well as **2**) biosynthesis.[7] However, recent evidence suggests that this enzyme may not play a direct role in C5a−C11a reduction but may be a coenzyme F_{420}:L-glutamate ligase that is essential in the biosynthesis of the F_{420} cofactor itself (Figure S1).[8] Initial bioinformatic analysis revealed that no F_{420}-binding enzyme is encoded in either the *oxy* or the *ctc* cluster.[3a,f] However, recent heterologous expression of the *oxy* cluster (spanning *otr*A to *otr*B), which resulted in the production of **1** in *Myxococcus xanthus*[9] and *Streptomyces lividans* K4−114,[4b] strongly suggests that all the enzymes required to convert **3** to **1** are encoded within the cluster. This therefore prompted us to examine the uncharacterized *oxy* genes.

OxyR is a small protein (16 kDa) encoded immediately adjacent, and in opposite polarity to *oxyS*, and the two are cotranscribed from the bidirectional promoter region (Figure S2).[10] A similar genetic arrangement of homologues of OxyS and OxyR is also observed in the *ctc* gene cluster. OxyR shares 63% and 64% similarities to CtcR from *ctc* cluster and DacO4 from the recently sequenced dactylocycline (*dac*) gene cluster, respectively.[4b,11] A new phylogenetic profiling method was recently used to uncover previously unassigned, F_{420}-containing enzymes in bacteria.[12] Intriguingly, bioinformatic analysis using these newly reannotated enzymes now shows OxyR, CtcR and DacO4 are predicted to use F_{420} as a cofactor. The up-to-date in silico analysis and the *oxyR*−*oxyS* genetic arrangement led us to examine the role of OxyR. We inactivated *oxyR* gene in the *oxy* pathway that is heterologously transplanted in *S. lividans* K4−114, which resulted in elimination of biosynthesis of **1** (Figure S3). No known intermediate leading to and including **3** was accumulated from this strain. This hinted that OxyR participates in the transformation of **3** to **1**, most likely following the C6 hydroxylation of **3** to **6** catalyzed by OxyS. The 1,3,5-triketo-containing **6** is known to be highly unstable, which may account for the lack of intermediates in the Δ*oxyR*
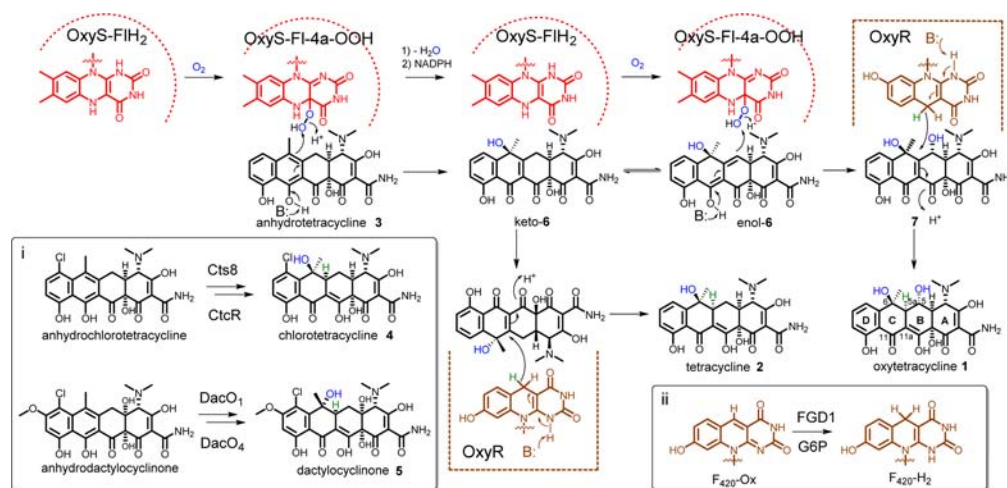
Figure 1. Proposed mechanisms of the transformations of **3** to **1** and **2**. The Fl-4a-OOH bound OxyS catalyzes the first hydroxylation at C6 of **3** to form **6**, which is in equilibrium between keto and enol forms. The latter is hydroxylated at C5 by the reoxidized OxyS-Fl-4a-OOH to form the intermediate **7**. Holo-OxyR with reduced F_{420} catalyzes the C5a−C11a reduction to afford the final product **1**. If C5 hydroxylation does not take place, OxyR reduces **6** into **2**. Insets: (i) Parallel oxidation and reduction steps that produce **4** and **5**; (ii) Regeneration of F_{420}-Ox to F_{420}-H_2 catalyzed by F_{420}-dependent glucose-6-phosphate dehydrogenase (*Mbt*-FGD1) using glucose-6-phosphate (G6P) as substrate.

strain. To probe the timing of OxyR, we constructed a recombinant *S. lividans* strain that overexpresses both OxyS and OxyR using the *ermE** promoter (Supplemental Methods), and **3** was then supplemented to a liquid culture of this strain as a substrate for biotransformation. Following 3 days of culturing, the production of **1** was detected (Figure S3), indicating that only OxyS and OxyR are sufficient to convert **3** to **1** in vivo. To investigate the role of OxyR in the pathway and whether it is indeed the F_{420}-dependent tetracycline dehydrogenase, we then turned to in vitro experiments using purified enzymes.

The polyhistidine-tagged OxyR was expressed and purified from *S. lividans* TK64 (Figure S4). OxyR purifies with a light-yellow color indicating that it is bound to a cofactor. Purified *holo*-OxyR was denatured, and the resulting yellow supernatant was subjected to LC-MS analysis. The analysis showed released compounds with UV absorption spectrum, retention time, and mass consistent with coenzyme F_{420} purified from *Mycobacterium smegmatis* cells (Figure S5).[13] This result hints that the small OxyR is the elusive F_{420}-dependent C5a−C11a reductase. To generate the reduced form of F_{420} cofactor (F_{420}-H_2) in situ (Figure 1, inset ii), the F_{420}-dependent glucose-6-phosphate dehydrogenase from *M. tuberculosis* (*Mtb*-FGD1) was expressed and purified from *M. smegmatis*.[14] When *holo*-OxyS purified from *Escherichia coli* (Figure S4) and *holo*-OxyR were added to **3** in the presence of NADPH and the F_{420} regeneration system, we detected the complete conversion of **3** to **1** and **2** (Figure 2e). This is therefore consistent with our in vivo result that OxyS and OxyR are sufficient to produce the mature tetracycline scaffold. The unexpected production of **1**, instead of **2**, as the major product in this assay indicates that the C5 hydroxylation step that converts **6** to **7** is also catalyzed by OxyS (Figure 1 and see discussion below). Recombinant OxyR purified from *E. coli* does not exhibit any yellow color and does not release F_{420} upon denaturation, as would be expected from the lack of F_{420} in *E. coli* metabolism.[15] This *apo*-OxyR, when reconstituted with F_{420}, along with *holo*-OxyS similarly catalyzed the conversion of **3** to **1** and **2** with a product ratio of 7:1 (Figure 2d).

Removal of OxyS from the reaction led to no conversion of **3** (Figure 2f), as expected since formation of the C5a−C11a
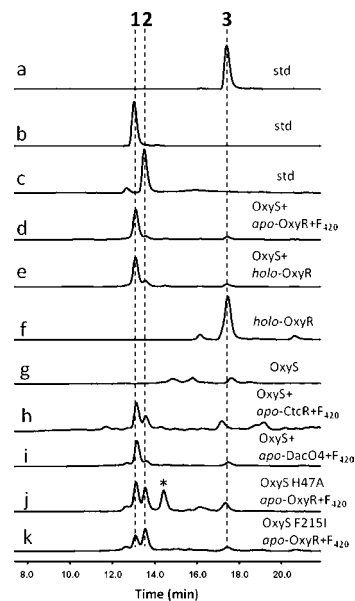
Figure 2. Analysis of OxyR and OxyS functions. The HPLC traces (270 nm) of the authentic compounds (a) **1**, (b) **2**, and (c) **3** and the enzymatic reaction products by (d) OxyS, *apo*-OxyR and F_{420}; (e) OxyS and *holo*-OxyR; (f) *holo*-OxyR only; (g) OxyS only; (h) OxyS, *apo*-CtcR and F_{420}; (i) OxyS, *apo*-DacO4 and F_{420}; (j) OxyS-H47A, *apo*-OxyR and F_{420}; (k) OxyS-F215I, *apo*-OxyR and F_{420}. Final concentrations are 20 μM OxyS, 20 μM OxyR, 100 μM **3**, and 2 mM NADPH. To regenerate the reduced form of F_{420}, 2 μM FGD1, 20 μM F_{420}, and 2 mM G6P are added. Asterisk indicates an uncharacterized compound with the same mass as **2**.

double bond requires C6 hydroxylation and dearomatization of the C ring of **3** by OxyS. Exclusion of OxyR from the reaction led to complete consumption of **3**, but no stable product can be isolated for characterization (Figure 2g). At very early time points (∼1 min), uncharacterized products with masses (m/z 443 $[M+H]^+$, m/z 459 $[M+H]^+$) consistent with those of singly and doubly hydroxylated products can be detected in the OxyS-only reaction mixture (Figure S6). However these products

rapidly degraded, in line with our observation that the Δ*oxyR S. lividans* strain does not accumulate any isolatable intermediates.

The mechanisms of the OxyS and OxyR reactions are shown in Figure 1. OxyS catalyzes the stereospecific hydroxylation of **3** at C6 via the oxidized OxyS-Fl-4a-OOH form using the monooxygenase mechanism.[16] We propose the resulting **6** can be released by OxyS and can be captured by OxyR to reduce the C5a−C11a double bond using the low-potential hydride provided by the F_{420}-H_2 cofactor and yield **2**. However, OxyS can recapture **6** and perform an additional hydroxylation with opposite stereochemistry at C5 to yield **7**. During their total synthesis of tetracycline, Myers and co-workers reported a C6 hydroperoxide analog of **6** that can equilibrate between ketone and enol forms at C11−C11a−C5a−C5, which confirms that vinylogous C5 proton in **6** is sufficiently acidic.[17] We propose that C5 hydroxylation of enol-**6** can also be initiated through the base-catalyzed proton extraction of the C11 hydroxyl. However, the C6-substituted and dearomatized **6** must bind in a different conformation in the active site of OxyS compared to that of **3**. This may account for the C5 carbanion attacking Fl-4a-OOH from the opposite face to give the flipped stereo-chemistry of the hydroxyl group at C5. The resulting **7** is then released and reduced by OxyR to yield **1**. The 8-hydroxy-7-desmethyl-5-deazariboflavin part of the oxidized F_{420} (F_{420}-Ox) is then reduced by *Mbt*-FGD1 using G6P as hydride donor (Figure 1, inset ii).

Our reconstitution of the final step of **1** biosynthesis raises questions with regard to the lack of C5 hydroxylation in the *ctc* or *dac* pathways (Figure 1, inset i). We examined the effect of substituting OxyR homologues from these pathways on product distribution from the in vitro assays. Both CtcR and DacO4 enzymes were purified in *apo* forms from *E. coli* (Figure S4) and reconstituted with F_{420} into the *holo* forms. Analysis of products showed that although **1** is still the dominant product, using CtcR or DacO4 decreased the ratio of **1** to **2** (Figure 2h,i). Notably when CtcR is used, the ratio is decreased to below 2:1. These mix and match assays showed that both CtcR and DacO4 are the F_{420}-dependent C5a−C11a reductase in the respective pathways and that compared to OxyR, CtcR displays a stronger affinity for **6** in competition with OxyS for the second hydroxylation step, albeit the latter still dominates to afford **1** as the major product.

We attempted to examine if OxyS homologues have differential abilities to catalyze the C5 hydroxylation step. Unfortunately, we were not able to obtain soluble forms of either Cts8 or DacO1 from *Streptomyces* and *E. coli*. Therefore, to understand the structural basis of the tandem hydroxylation reactions and to guide mutational approaches, we determined the crystal structure of OxyS in complex with oxidized flavin (Fl_{ox}) to 2.6 Å resolution (see Table S1 for statistics). The monomeric OxyS is comprised of three structural domains, including the FAD-binding domain (residues 1−175 and 271−389), the middle domain (residues 176−270), and the C-terminal thioredoxin-like domain (residues 390−503) (Figure 3). The overall structure of OxyS is similar to other FAD-dependent monooxygenases found in the pathways of aromatic polyketides, including aklavinone-11 hydroxylase RdmE (PDB ID: 3ihg) from the rhodomycin pathway[18] as well as PgaE (PDB: 2qa1) and CabE (PDB: 2qa2) from angucycline pathways (Figure S7).[19] Attempts to obtain OxyS structures bound to **3** were not successful. To model likely interactions between **3** and the substrate binding pocket of OxyS, we performed structural alignment with RdmE in complex with the
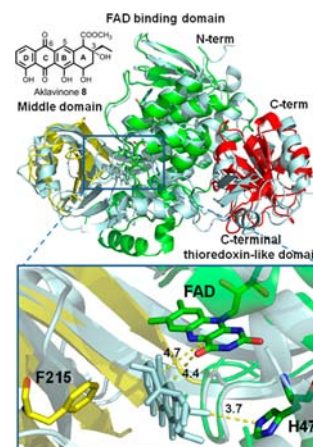
Figure 3. Overall structure alignment of OxyS with the complex of RdmE cocrystallized with aklavinone **8** (pale cyan, PDB ID: 3ihg). RdmE is shown in pale cyan, while OxyS is colored according to domains. The RMSD is 1.51 Å for 282 matching α carbons. The magnified region of the catalytic pocket indicates possible orientation of the substrate **3** or **6** using the cocrystallized **8** (shown in pale cyan). Mutation of H47A and F215I increased the amount of **2** to **1**.

cocrystallized, aklavinone **8** (Figures 3 and S9). Using the superimposed structures of OxyS and RdmE (the RMSD is 1.51 Å for 282 matching α carbons) and the coordinates of **8**, we can propose a putative binding pocket and binding orientation for **3**. The tetracycline substrate is anchored in a narrow hydrophobic cleft at the interface between the FAD-biding and the middle domains, as indicated for **8** in Figure 3. The middle domain provides a hydrophobic and aromatic patch (Trp211-Leu217, OxyS numbering, for alignment see Figure S7) against the D and C rings of **8**. On the other side of the pocket, the well conserved patch PAGG helps to position the substrate with respect to the FAD isoalloxazine ring. As shown in Figure 3 for **8** and can be envisioned for **3**, the planar C−D rings are perpendicular to the isoalloxazine ring of Fl_{ox}, with the C6 carbon placed 4.7 Å away from the bridgehead C4a of Fl_{ox}. Similarly, the C5 carbon is also located within striking distance (4.4 Å) of C4a, which may explain how OxyS can hydroxylate both positions. However, in order to achieve the opposite stereochemical outcomes, substrates **3** and **6** must be tilted with respect to the FAD ring to facilitate attack of C6 and C5 on Fl-C4a-OOH from the opposite faces. Hence it is likely that slight perturbation in the geometry of the binding pocket can alter the ability and stereoselectivity of OxyS in catalyzing the hydroxylation steps.

To test this hypothesis, we further generated a modeled configuration of **3** in the active site of OxyS based on the D- and C-ring coordinates of **8**. This is to account for the nonplanar nature of the A and B rings in **3** (Supplemental Methods and Figure S9). Comparison of the modeled positions of **8** and **3** led us to mutate His47 and Phe215, which appear to be in close contact with the substrates (Figures 3 and S9). The N1 of His47 imidazole side chain is located 3.7 Å away from the C3 oxygen atom in **8**, suggesting it might hydrogen bond to the same hydroxyl position in the A ring of **3** and **6**. When the assay was performed in the presence of a His47Ala mutant of OxyS (Figure S4), a decreasing ratio of **1** to **2** was observed. This implies that disrupting the possible hydrogen-bonding inter-actions can indeed lead to a repositioning of the substrate and to a decrease in the efficiency of the C5 hydroxylation step. Interestingly, we also observed the emergence of a new product

from the assay that has similar UV and identical mass (m/z 445 [M+H]$^+$) as **2** (Figures 2j and S8). Although the structure of the compound cannot be determined due to low amounts produced from the in vitro assay, it is possible that this is the 6R−OH analog of **2** formed from the altered binding of **3** in the mutant active site.

On the other hand, Phe215 is located near the entrance of the active site, and the phenyl side chain is positioned close to the C ring. The proximity of the bulky side chain may also play a role in orienting the position of **3** and **6** in the active site with respect to Fl-4a-OOH. To investigate the role of this residue, we made the mutation of Phe215Ile. Surprisingly, the slight decrease in the volume of the side chain at position 215 led to dramatic changes in the product ratio of **1:2** (Figure 3k), in which the amount of **2** now exceeded that of **1**. Although these mutagenesis studies were based on a structural alignment using the different substrate **8**, and the exact roles of these residues may differ during catalysis, it is clear that the ability of OxyS to hydroxylate both C6 and C5 has been intricately tuned during evolution. In Cts8 and DacO1, variations in the active-site configuration can lead to the exclusive production of the C6 hydroxylated products as well as the opposite stereochemistry at C6 observed in dactylocyclinone (Figure 1, inset i). Similarly, the additional substitutions in D rings of anhydrochlorotetracycline and anhydrodactylocyclinone, such as the C7 chlorine and C8 methoxy, can further lead to differences in substrate orientation in the corresponding active sites.

In conclusion, we showed that OxyR, CtcR, and DacO4 are F$_{420}$-dependent reductases catalyzing the key C5a−C11a reduction step in respective tetracycline biosynthetic pathways. Our in vitro results demonstrate that secondary metabolic pathways in actinobacteria can use F$_{420}$ in natural product biosynthesis, which expands the utility of this cofactor beyond a nicotinamide equivalent in methogenic archaea[20] and mycobacteria.[12] This is in line with the isolation of F$_{420}$ from the fermentation broths of numerous actinomycetes.[21] Other OxyR-like enzymes in secondary metabolism exist in the database, including ActVA2 (64% similarity), an enzyme of unknown function from the actinorhodin biosynthetic pathway.[22] Using structural-guided mutagenesis, we showed that OxyS is responsible for both C6 and C5 hydroxylation steps during the conversion of **3** to **1**. While substrate specificities of OxyS and OxyR are important for the observed relative ratio of **1** to **2**, it is the unexpected ability of OxyS to catalyze the C5 hydroxylation that results in formation of **1** in the *oxy* pathway.

ASSOCIATED CONTENT

S **Supporting Information**

Experimental details and characterization data. This information is available free of charge via the Internet at http://pubs.acs.org.

AUTHOR INFORMATION

Corresponding Author
yitang@ucla.edu

Notes
The authors declare no competing financial interest.

ACKNOWLEDGMENTS

REFERENCES

(1) (a) Chopra, I.; Roberts, M. *Microbiol. Mol. Biol. Rev.* **2001**, *65*, 232. (b) Hertweck, C.; Luzhetskyy, A.; Rebets, Y.; Bechthold, A. *Nat. Prod. Rep.* **2007**, *24*, 162.

(2) (a) Thaker, M.; Spanogiannopoulos, P.; Wright, G. D. *Cell. Mol. Life Sci.* **2010**, *67*, 419. (b) Nelson, M. L.; Levy, S. B. *Ann. N.Y. Acad. Sci.* **2011**, *1241*, 17.

(3) (a) Zhang, W.; Ames, B. D.; Tsai, S. C.; Tang, Y. *Appl. Environ. Microbiol.* **2006**, *72*, 2573. (b) Zhang, W.; Watanabe, K.; Cai, X.; Jung, M. E.; Tang, Y.; Zhan, J. *J. Am. Chem. Soc.* **2008**, *130*, 6068. (c) Béhal, V.; Hoštálek, Z.; Vaněk, Z. *Biotechnol. Lett.* **1979**, *1*, 177. (d) Binnie, C.; Warren, M.; Butler, M. J. *J. Bacteriol.* **1989**, *171*, 887. (e) Butler, M. J.; Gedge, B. N. *Biotechnol. Tech.* **1989**, *4*, 235. (f) Hunter, I. S.; Hill, R. A. In *Biotechnology of Antibiotics*; 2 ed.; Strohl, W. R., Ed.; Marcel Dekker: New York, 1997, p 659.

(4) (a) Peric-Concha, N.; Borovicka, B.; Long, P. F.; Hranueli, D.; Waterman, P. G.; Hunter, I. S. *J. Biol. Chem.* **2005**, *280*, 37455. (b) Wang, P.; Kim, W.; Pickens, L. B.; Gao, X.; Tang, Y. *Angew. Chem., Int. Ed.* **2012**, *51*, 11136.

(5) Brodersen, D. E.; Clemons, W. M., Jr.; Carter, A. P.; Morgan-Warren, R. J.; Wimberly, B. T.; Ramakrishnan, V. *Cell* **2000**, *103*, 1143.

(6) (a) Mccormick, J. R. D.; Hirsch, U.; Sjolander, N. O.; Doerschuk, A. P. *J. Am. Chem. Soc.* **1960**, *82*, 5006. (b) Rhodes, P. M.; Winskill, N.; Friend, E. J.; Warren, M. *J. Gen. Microbiol.* **1981**, *124*, 329. (c) Walsh, C. *Acc. Chem. Res.* **1986**, *19*, 216.

(7) Nakano, T.; Miyake, K.; Endo, H.; Dairi, T.; Mizukami, T.; Katsumata, R. *Biosci. Biotechnol. Biochem.* **2004**, *68*, 1345.

(8) Nocek, B.; Evdokimova, E.; Proudfoot, M.; Kudritska, M.; Grochowski, L. L.; White, R. H.; Savchenko, A.; Yakunin, A. F.; Edwards, A.; Joachimiak, A. *J. Mol. Biol.* **2007**, *372*, 456.

(9) Stevens, D. C.; Henry, M. R.; Murphy, K. A.; Boddy, C. N. *Appl. Environ. Microbiol.* **2010**, *76*, 2681.

(10) McDowall, K. J.; Thamchaipenet, A.; Hunter, I. S. *J. Bacteriol.* **1999**, *181*, 3025.

(11) Ryan, M. J., *U.S. Patent* 5,965,429; Wyeth Holdings Corporation: Madison, NJ, 1999.

(12) Selengut, J. D.; Haft, D. H. *J. Bacteriol.* **2010**, *192*, 5788.

(13) Bashiri, G.; Rehan, A. M.; Greenwood, D. R.; Dickson, J. M.; Baker, E. N. *PLoS One* **2010**, *5*, e15803.

(14) (a) Purwantini, E.; Daniel, L. *J. Bacteriol.* **1996**, *178*, 2861. (b) Bashiri, G.; Squire, C. J.; Moreland, N. J.; Baker, E. N. *J. Biol. Chem.* **2008**, *283*, 17531.

(15) Eirich, L. D.; Vogels, G. D.; Wolfe, R. S. *J. Bacteriol.* **1979**, *140*, 20.

(16) Walsh, C. T.; Wencewicz, T. A. *Nat. Prod. Rep.* **2013**, *30*, 175.

(17) Charest, M. G.; Siegel, D. R.; Myers, A. G. *J. Am. Chem. Soc.* **2005**, *127*, 8292.

(18) Lindqvist, Y.; Koskiniemi, H.; Jansson, A.; Sandalova, T.; Schnell, R.; Liu, Z.; Mantsala, P.; Niemi, J.; Schneider, G. *J. Mol. Biol.* **2009**, *393*, 966.

(19) Koskiniemi, H.; Metsa-Ketela, M.; Dobritzsch, D.; Kallio, P.; Korhonen, H.; Mantsala, P.; Schneider, G.; Niemi, J. *J. Mol. Biol.* **2007**, *372*, 633.

(20) Graham, D. E.; White, R. H. *Nat. Prod. Rep.* **2002**, *19*, 133.

(21) (a) Coats, J. H.; Li, G. P.; Kuo, M. S.; Yurek, D. A. *J. Antibiot. (Tokyo)* **1989**, *42*, 472. (b) Kuo, M. T.; Yurek, D. A.; Coats, J. H.; Li, G. P. *J. Antibiot. (Tokyo)* **1989**, *42*, 475.

(22) Caballero, J. L.; Martinez, E.; Malpartida, F.; Hopwood, D. A. *Mol. Gen. Genet.* **1991**, *230*, 401.